Detuning-modulated composite pulses for high-fidelity robust quantum control

Elica Kyoseva,[1,2,3,*] Hadar Greener,[2,3] and Haim Suchowski[2,3]
[1]*Institute of Solid State Physics, Bulgarian Academy of Sciences, 72 Tsarigradsko Chaussee, 1784 Sofia, Bulgaria*
[2]*Condensed Matter Physics Department, School of Physics and Astronomy, Tel Aviv University, Tel Aviv 69978, Israel*
[3]*Center for Light-Matter Interaction, Tel Aviv University, Tel Aviv 69978, Israel*

(Received 10 September 2018; revised manuscript received 1 August 2019; published 25 September 2019)

We introduce a control method for off-resonant robust quantum information processing suited for quantum integrated photonics. We utilize detunings as control parameters to derive a family of composite pulses for high-fidelity complete population transfer. The presented detuning-modulated composite sequences can be implemented within the decay lifetime of the qubit and correct for control inaccuracies in various parameters including pulse strength, duration, detuning, phase jitter, Stark shift, and unwanted frequency chirps. We implement the proposed robust sequences in an integrated photonics platform to achieve complete light transfer insensitive to fabrication errors.

DOI: 10.1103/PhysRevA.100.032333

I. INTRODUCTION

Quantum information processing (QIP) relies on high-fidelity quantum state preparation and transfer. This presents a challenge in practical realizations of QIP where the admissible error of quantum operations is smaller than 10^{-4} [1]. Thus small systematic errors due to imperfections in fabrication or in the experimental control knobs reduce the fidelity of state transfer below the fault-tolerant threshold. A powerful tool to correct for systematic errors is composite pulses (CPs), which were initially developed in the field of nuclear magnetic resonance [2–9]. A composite pulse is a sequence of pulses with different areas and/or phases that implement accurate and robust quantum gates. To this end, CPs are designed for resonant or adiabatic interactions with complex coupling parameters [10–12] and were successfully used to achieve complete population transfer (CPT) in quantum systems in both rf and ultrashort pulses [13].

More recently, CPs found applications in matching higher harmonic generation processes [14] and in designing polarization rotators [15,16], as well as in QIP realizations including trapped ions [17] and atomic systems [18,19]. Another promising candidate for advancing QIP technologies is integrated photonic circuits due to their scalability and on-chip integration capacity [20–22]. However, to date, the gate fidelity remains below the QIP threshold due to unavoidable fabrication errors. CPs have not been previously used to correct for such errors as existing CP sequences require control of the phase of the coupling, whereas in integrated photonic circuits it is a real parameter. The present research is the first to address this limitation and to derive CPs that can be used in any qubit architecture including integrated photonics.

In this paper, we introduce the first composite sequences designed for off-resonant robust qubit inversion. We realize the desired high-fidelity population transfer by suitably choosing the detuning parameters while maintaining constant coupling throughout the constituent pulses. The presented general approach to derive detuning-modulated composite pulses of an arbitrary length N has a minimal pulse overhead and robust transfer is realized even for $N = 2$. In our analysis we consider a generic qubit which has many physical realizations including atomic and photonic systems (Fig. 1). We show that our sequences are stable to inaccuracies in various systematic parameters—coupling strength, duration, phase jitter, and resonance offsets—and achieve fidelities well above the QIP gate error threshold within the temporal lifetime of the system. Finally, we lay out the general recipe to implement the presented detuning-modulated composite sequences in integrated photonic systems for broadband high fidelity optical switching.

II. DETUNING-MODULATED COMPOSITE PULSES

The dynamics of a qubit $\{|1\rangle, |2\rangle\}$ driven coherently by an external electromagnetic field [Fig. 1(a)] is governed by the Schrödinger equation

$$i\hbar\partial_t \begin{bmatrix} c_1(t) \\ c_2(t) \end{bmatrix} = \frac{\hbar}{2} \begin{bmatrix} -\Delta(t) & \Omega(t) \\ \Omega^*(t) & \Delta(t) \end{bmatrix} \begin{bmatrix} c_1(t) \\ c_2(t) \end{bmatrix}. \quad (1)$$

Here, $[c_1(t), c_2(t)]^{\mathrm{T}}$ is the probability amplitudes vector, $\Omega(t)$ is the Rabi frequency of the transition, and $\Delta(t) = (\omega_0 - \omega)$ is the real-valued detuning between the laser frequency ω and the Bohr transition frequency of the qubit ω_0. In what follows, we assume $\Omega(t)$ and $\Delta(t)$ real and constant, which is well suited for the foreseen implementation in coupled waveguides and in optical elements for generating higher harmonics. However, we note that our composite sequences can also be implemented in physical systems with complex $\Omega(t)$.

*elkyoseva@gmail.com

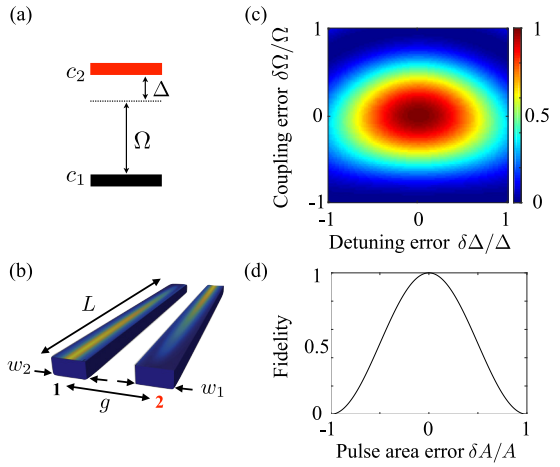

FIG. 1. Coherent qubit dynamics. Qubit realization in (a) an atomic system driven by a field with Rabi frequency Ω and detuning Δ and in (b) coupled waveguides of widths w_1 and w_2 at a distance g. (c) Population transfer fidelity as a function of detuning and coupling errors. (d) Resonant Rabi oscillations. The permissible gate infidelity is $<10^{-4}$.

The unitary propagator corresponding to Eq. (1) is found according to $U(t,0) = e^{-i/\hbar \int_0^t H(t)dt}$ and reads

$$U(\delta t) = \begin{bmatrix} \cos\left(\frac{A}{2}\right) + i\frac{\Delta}{\Omega_g}\sin\left(\frac{A}{2}\right) & -i\frac{\Omega}{\Omega_g}\sin\left(\frac{A}{2}\right) \\ -i\frac{\Omega}{\Omega_g}\sin\left(\frac{A}{2}\right) & \cos\left(\frac{A}{2}\right) - i\frac{\Delta}{\Omega_g}\sin\left(\frac{A}{2}\right) \end{bmatrix}. \tag{2}$$

Here, $\Omega_g = \sqrt{\Omega^2 + \Delta^2}$ is the generalized Rabi frequency and $A = \Omega_g \delta t$ is the pulse area with $\delta t = (t - t_0)$ being the pulse duration. The propagator $U(\delta t)$ evolves the state of the qubit from the initial time t_0 to the final time t according to $\mathbf{c}(t) = U(\delta t)\mathbf{c}(t_0)$. If the initial state of the qubit at t_0 is $|1\rangle$, the population of the excited state $|2\rangle$ at time t is given by the modulus squared of the off-diagonal propagator element $|U_{12}(\delta t)|^2$.

We assume the most general composite pulse sequence comprising N individual off-resonant pulses with Rabi frequencies Ω_n and detunings Δ_n. Given the individual pulse propagator $U_n(\delta t_n)$ from Eq. (2), the propagator for the total composite pulse sequence is expressed by the product

$$U^{(N)}(T,0) = U_N(\delta t_N)\, U_{N-1}(\delta t_{N-1}) \ldots U_1(\delta t_1), \tag{3}$$

where $\delta t_n = (t_n - t_{n-1})$ is the duration of the nth pulse ($t_0 = 0$ and $t_N \equiv T$). Below, we focus on the case of ingredient π pulses, i.e., $A_n = A = \pi$, which is easily realized by setting the pulse durations according to $\delta t_n = \pi/\sqrt{\Omega_n^2 + \Delta_n^2}$.

A. General propagator matrix

We require that the composite sequence produces a preselected single-qubit rotation T on the Bloch sphere at an angle θ,

$$T = \begin{bmatrix} \cos\theta & -i\,\sin\theta \\ -i\,\sin\theta & \cos\theta \end{bmatrix}. \tag{4}$$

That is, at the end of the pulse sequence the propagator from Eq. (3) should implement the target T. The exact form of the off-diagonal element of the composite propagator for an arbitrary *even* $N = 2n$ *pulse sequence* is given by

$$\left|U_{12}^{(2n)}(T,0)\right| = \prod_{s=1}^{2n} \frac{|\Omega_s|}{\sqrt{\Omega_s^2 + \Delta_s^2}} \Bigg| \sum_{i=1}^{2n} (-1)^{i+1} \frac{\Delta_i}{\Omega_i} + \sum_{i<j<k=1}^{2n} (-1)^{i+j+k} \frac{\Delta_i}{\Omega_i}\frac{\Delta_j}{\Omega_j}\frac{\Delta_k}{\Omega_k} + \cdots + \sum_{i<\cdots<m=1}^{2n} (-1)^{i+\cdots+m+1} \underbrace{\frac{\Delta_i}{\Omega_i} \cdots \frac{\Delta_m}{\Omega_m}}_{2n-1} \Bigg|, \tag{5}$$

while for an *odd* $N = (2n+1)$ *pulse sequence* by

$$\left|U_{12}^{(2n+1)}(T,0)\right| = \prod_{s=1}^{2n+1} \frac{|\Omega_s|}{\sqrt{\Omega_s^2 + \Delta_s^2}} \Bigg| 1 + \sum_{i<j=1}^{2n+1} (-1)^{i+j+1} \frac{\Delta_i}{\Omega_i}\frac{\Delta_j}{\Omega_j} + \sum_{\substack{i<j< \\ k<l=1}}^{2n+1} (-1)^{i+j+k+l} \frac{\Delta_i}{\Omega_i}\frac{\Delta_j}{\Omega_j}\frac{\Delta_k}{\Omega_k}\frac{\Delta_l}{\Omega_l} + \cdots + \sum_{i<\cdots<m=1}^{2n+1} (-1)^{i+\cdots+m+1} \underbrace{\frac{\Delta_i}{\Omega_i} \cdots \frac{\Delta_m}{\Omega_m}}_{2n} \Bigg|. \tag{6}$$

We require that $|U_{12}^{(N)}(T,0)| = |\sin\theta|$.

B. Complete population transfer

Below we focus on providing the protocol for the derivation of composite sequences, which produce a robust complete population inversion. The same protocol can be followed for any other rotation angle θ and we provide an example for $\theta = \pi/2$ in the Appendix.

For target $\theta = \pi$, we require that the modulus squared of the off-diagonal element from Eq. (3) should be equal to 1, $|U_{12}^{(N)}(T,0)| = 1$. To fulfill this condition we use the set of detunings $\{\Delta_n\}$ as *free control parameters*. We find that for a complete population inversion they need to obey a general analytical condition depending on the parity of N. For an even $N = 2n$, the condition is

$$1 + \sum_{i<j=1}^{2n} (-1)^{i+j+1} \frac{\Delta_i}{\Omega_i}\frac{\Delta_j}{\Omega_j} + \cdots + \sum_{i<\cdots<m=1}^{2n} (-1)^{i+\cdots+m+1} \underbrace{\frac{\Delta_i}{\Omega_i} \cdots \frac{\Delta_m}{\Omega_m}}_{2n \text{ times}} = 0, \tag{7}$$

while for an odd $N = (2n+1)$ it reads

$$\sum_{i=1}^{2n+1} (-1)^{i+1} \frac{\Delta_i}{\Omega_i} + \sum_{i<j<k=1}^{2n+1} (-1)^{i+j+k} \frac{\Delta_i}{\Omega_i}\frac{\Delta_j}{\Omega_j}\frac{\Delta_k}{\Omega_k} + \cdots + \sum_{i<\cdots<m=1}^{2n+1} (-1)^{i+\cdots+m+1} \underbrace{\frac{\Delta_i}{\Omega_i} \cdots \frac{\Delta_m}{\Omega_m}}_{(2n+1) \text{ times}} = 0. \tag{8}$$

Note that the above Eq. (7) or (8), depending on the parity of the composite pulse, is the only condition that the detuning and coupling parameters need to fulfill in order to realize a population inversion in the system.

The next step in our protocol is to find which subset of the solutions to Eqs. (7) and (8) produce an excitation profile that is maximally robust to variations in the pulse area A at selected value(s) of A. This is achieved mathematically by nullifying the even derivatives of the propagator element $\frac{\partial^k}{\partial A^k}|U_{12}^{(N)}(T,0)|^2$ at $A=\pi$. Note that the odd derivatives are always equal to zero. Thus for a *first-order CP* realizing a robust composite sequence that corrects for imperfections in the pulse area we need to nullify the second derivative, while for a *second-order CP*—the second and the fourth derivatives simultaneously. Note, that in contrast to previous works [10,11,18], the pulse area A for an off-resonant pulse is a function of all systematic parameters—pulse duration, amplitude, and detuning—and thus the detuning-modulated composite pulses presented here are *robust against various systematic errors*.

C. First-order composite pulses: Sign-alternating Δs

In the following we provide analytical solutions for broadband pulse sequences of arbitrary lengths N. In order to obtain the elegant analytical solutions for arbitrary N presented below we assume that the detuning and coupling parameters values are not completely arbitrary but they have equal ratios $|\frac{\Delta_i}{\Omega_i}|=|\frac{\Delta_j}{\Omega_j}|,\ \forall i,j$. The uncovered pulse symmetries represent a powerful analytical quantum control tool and allow for finding sequences of arbitrary lengths in a straightforward manner. The presented sequences will be straightforward to realize in NMR and in coupled waveguide qubits.

Our first-order composite pulse parameters are antisymmetric along their length, i.e., $\frac{\Delta_i}{\Omega_i}=-\frac{\Delta_{i+1}}{\Omega_{i+1}}\equiv\xi$ for $i=(1,\ldots,N-1)$. The rationale behind this is that the composite sequence needs to produce a change in the path of the state vector on the Bloch sphere (see the inset of Fig. 5). Then, the CPT conditions Eqs. (7) and (8) can be rewritten as the polynomial

$$\sum_{s=0}^{n}(-1)^s\binom{N}{N-2s}\xi^{N-2s}=0, \tag{9}$$

which is valid for both even $N=2n$ and odd $N=(2n+1)$ sequences. The roots of this polynomial provide the values of δ for which a complete population transfer is achieved and moreover $\frac{\partial^2}{\partial A^2}|U_{12}^{(N)}|^2$ at $A=\pi$ is nullified. For a flat-top broadband composite sequence we choose the root that minimizes the fourth derivative $\frac{\partial^4}{\partial A^4}|U_{12}^{(N)}|^2$ at $A=\pi$ (the polynomial is a symmetric function of ξ). Finally, we find that first-order detuning-modulated CPs of length N are realized for δ equal to the largest (in absolute value) root of the polynomial Eq. (9). In Table I we present the first several examples for CPs.

D. Second-order composite pulses: Antisymmetric Δs

Second-order CPs are of odd pulse length, $N=(2n+1)$, and similar to the first-order ones the ratios of the detunings and couplings are equal and antisymmetric with respect to the length of the pulse. That is, $\frac{\Delta_i}{\Omega_i}=-\frac{\Delta_{N+1-i}}{\Omega_{N+1-i}}\equiv\xi$, while the detuning of the middle pulse is $\Delta_{n+1}=0$. This antisymmetric arrangement fulfills the CPT condition Eq. (8) automatically and the second derivative is zero as it is proportional to the diagonal element of the propagator. To achieve a higher fidelity of the CPs we need to also nullify the fourth derivative $\frac{\partial^4}{\partial A^4}|U_{12}^{(N)}(T,0)|^2$ at $A=\pi$ and minimize the sixth. This task is simple numerically and in Table II we present a few examples of second-order CPs, which can easily be extended to large odd N.

TABLE I. First-order detuning-modulated CPs.

N	$\pm\left(\frac{\Delta_1}{\Omega_1},\frac{\Delta_2}{\Omega_2},\ldots\right)$
2	$(1,-1)$
3	$(1,-1,1)\sqrt{3}$
4	$(1,-1,1,-1)(\sqrt{2}+1)$

The above presented approach of tailoring the propagator element and its derivatives to achieve robustness against systematic parameters can be extended to implement other gates, i.e., create equal superposition between the states. In this case the propagator elements squared from (7) and (8) should be equal to $1/2$ and the derivatives with respect to any chosen systematic parameter should be nullified accordingly.

III. ROBUSTNESS OF THE DETUNING-MODULATED SEQUENCES

A. Pulse area errors and phase jitter

The infidelities of the first- and second-order composite sequences as a function of errors in the target pulse area are shown in Fig. 2. For easy reference, we include the fidelity of a resonant pulse and the QI gate error threshold [1]. Note that the infidelity of the population transfer is well below the QI benchmark even for $\delta A/A$ larger than 10% as compared to less than 1% for a resonant excitation. We achieve approximately an order of magnitude improvement in the error tolerance by adding a single pulse (first-order CP) and 1.5 orders of magnitude by adding two extra pulses (second-order CP). The pulse overhead scales as N, which is significantly better than that of previous proposals ($2N$) [10–12]. In our analysis we also allowed for Gaussian errors of 10% in the individual pulse areas and averaged over 100 times (with dashed curves). Note that any other first- and second-order pulses have similar robustness to the ones we show here as they nullify up to the same derivative of the propagator element and, for compactness, we have omitted them. Finally, we relaxed the assumption of real couplings Ω and allowed for a random

TABLE II. Second-order detuning-modulated CPs.

N	$\pm\left(\frac{\Delta_1}{\Omega_1},\frac{\Delta_2}{\Omega_2},\ldots,0,\ldots,\frac{\Delta_{N-1}}{\Omega_{N-1}},\frac{\Delta_N}{\Omega_N}\right)$
3	$(1,0,-1)\,2.5425$
5	$(1,-1,0,1,-1)\,5.09027$
7	$(1,-1,1,0,-1,1,-1)\,7.6375$

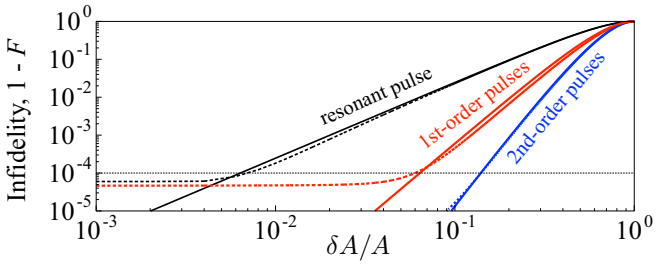

FIG. 2. Infidelity of the shortest first- (red) and second-order (blue) CPs vs area errors with (dashed curves) and without (solid curves) Gaussian noise of 10% in A averaged over 100 times. The point-dash blue curve shows the second-order pulse with a random phase error of 1%. The black curve shows the infidelity of a single resonant pulse and we also show the 10^{-4} QIP infidelity threshold.

phase jitter of 1% in the second-order pulse (dashed blue). We note that the error correction of our CPs is largely unaffected by such inaccuracies.

B. Detuning and coupling errors

We further examine the robustness of the detuning-modulated composite sequences in the presence of simultaneous detuning and coupling errors and show the population transfer fidelity in Fig. 3(a). We present the contour plots of the fidelity of the first-order (left) and second-order (right) CPs of length $N = 2$ and 3, respectively. Note that the contour plots for any other pulses from their respective families look similar. The area where the fidelity is above 90% is increased significantly as compared to that of a resonant pulse [Fig. 1(c)]. We also identify areas in the parameter space where the fidelity exhibits a notable stability against either detuning $\delta\Delta_i/\Delta_i$ or coupling $\delta\Omega/\Omega$ errors and mark them by horizontal and vertical cut lines in the contour plots. We zoom in on them in Figs. 3(b) and 3(c) and observe an increased robustness vs detuning and coupling errors.

C. In the presence of relaxation

As composite sequences require longer implementation times, it is important to test their fidelity against the lifetime of the system. Given relaxation, we substitute $\Delta \to (\Delta - i\gamma)$ in the diagonal elements of the Hamiltonian (1), and find the probability amplitude of each state according to $|c_i(t)|^2 e^{-\gamma t/2}$, where the relaxation time is $T_1 = \gamma^{-1}$. It is known that for free decay T_1 is independent of T_2 and there is an upper limit to the decoherence rate $T_2 \leqslant 2T_1$ [23,24]. We show the robustness of the population transfer with respect to γ in Fig. 4 where we have used experimentally reported decoherence values (Refs. [25–28]) to allow for γ of the order of Ω. The above analysis shows that the detuning-modulated sequences are a powerful tool for a robust qubit inversion even in the presence of decay or decoherence and that their implementation time is well within the decay time of the qubit.

IV. REALIZATION IN COUPLED WAVEGUIDES

The detuning-modulated CPs offer a unique solution to overcome inaccuracies in fabrication in integrated photonic

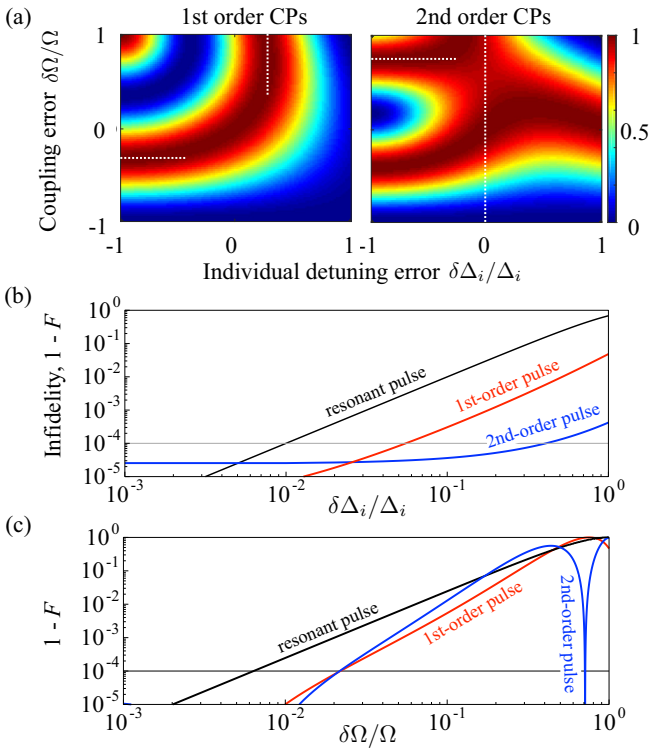

FIG. 3. Robustness of first- (left) and second-order (right) detuning-modulated sequences vs detuning and coupling errors. (a) Contour plots of the fidelity vs errors in both $\delta\Delta_i/\Delta_i$ and $\delta\Omega/\Omega$. The error tolerance is increased significantly as compared to the contour plot of a single resonant pulse, shown in Fig. 1(c). The infidelity, $1 - F$, along the horizontal (b) and vertical (c) cut lines from the contour plots from (a), where first-order pulses are in red and second-order pulses are represented with blue. For easy reference we show the 10^{-4} QIP infidelity threshold and the resonance pulse infidelity with black.

circuits. In Fig. 1(b), we show two evanescently coupled optical waveguides at a distance g measured from their center lines. Within the coupled-mode approximation [29], the amplitudes of the fundamental modes in the waveguides obey an equation analogous to Eq. (1) where the coupling is $\Omega = a\, e^{-bg}$ (a and b are material and geometry dependent). For constant g, Ω is also constant throughout the length. The system is on resonance if the waveguides have identical geometries; otherwise, there is a real-valued phase mismatch $\Delta = (\beta_1 - \beta_2)/2$ with $\beta_{1,2}$ being the respective propagation constants.

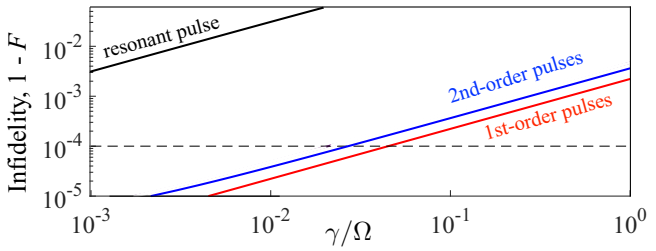

FIG. 4. Infidelity, $1 - F$, in log scale vs the decay rate in units of Ω for $N = 2$ first- and $N = 3$ second-order composite sequences and for a resonant pulse in red, blue, and black, respectively.

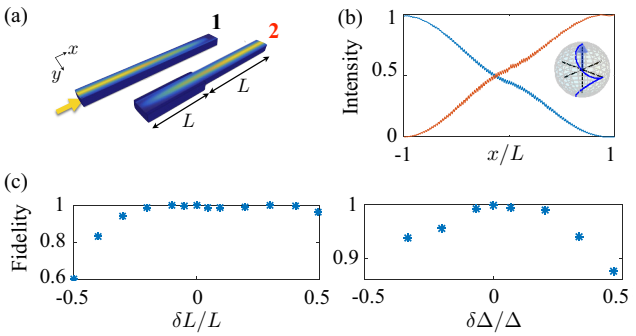

FIG. 5. Complete light transfer in a first-order $N = 2$ detuning-modulated composite waveguide coupler. (a) An out-of-scale schematic of the waveguide design with EME calculation. Light is initially injected in waveguide 1 and is then robustly transferred to waveguide 2. (b) Light intensity of waveguide 1 (blue, initially populated) and waveguide 2 (red, initially empty) vs normalized propagation length. The inset shows the path of the system's state vector on the Bloch sphere during the evolution. (c) Fidelity of the light transfer vs errors in (left) the propagation length L and (right) the target phase mismatch Δ.

Thus our sequences can be implemented by changing the waveguides' widths such that there are step changes in Δ along the length.

Figure 5(a) is an out-of-scale schematic of the $N = 2$ first-order CP in coupled waveguides of length $2L$. The width of waveguide 1, w_1, is fixed, while the width of waveguide 2 changes midlength from $1.034w_1$ to $0.966w_1$, realizing the required step change in Δ in Si on SiO_2 configuration. By employing an eigenmode expansion (EME) solver, we simulate the light propagation along the waveguides. We plot the light intensities in Fig. 5(b) along with the Bloch sphere path of the state vector. We realize a complete light switching and test its robustness to errors in the phase mismatch $\delta\Delta/\Delta$ and in the propagation length $\delta L/L$, shown in Fig. 5(c). We observe high fidelity light transfer in excellent agreement with the theoretical calculations (Figs. 2 and 3). Finally, in Fig. 6 we show light switching for $N = 3$ composite waveguides based on first- and second-order sequences.

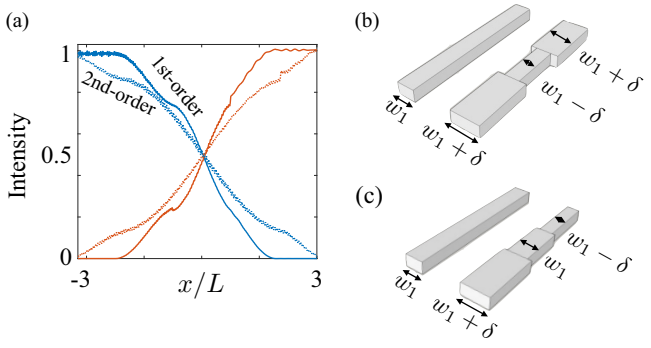

FIG. 6. (a) Light intensity as a function of normalized length of two composite waveguide couplers: one with first-order design as shown in (b) and one with second-order design as shown in (c). The light intensity of the initially populated waveguides [with blue curves in (a) starting from 1] is robustly transferred to the other waveguide [with red curves in (a) starting from zero].

V. CONCLUSIONS

We introduced a set of detuning-modulated composite pulse sequences that are robust to inaccuracies in various systematic parameters including duration, coupling strength, and off-resonance errors well within the system's lifetime. The control knobs, which we utilized to achieve broadband population transfer, are the detuning parameters of the constituent pulses, while the coupling constants remain unchanged. We achieved an inversion gate fidelity above the QI threshold vs errors of several percents in the pulse area for a sequence of only two constituent pulses and vs errors of over 10% for three constituent pulses. The presented composite pulses are radically different compared to existing composite sequences, which assume complex coupling parameters and modify their phases. Thus we believe that our analytical solutions will be the cornerstone for quantum information protocols in practical realization of high-fidelity quantum computing in integrated photonic circuits.

ACKNOWLEDGMENTS

E.K. acknowledges financial support from the European Union's Horizon 2020 research and innovation programme under the Marie Skłodowska-Curie Grant agreement No. 705256–COPQE. H.G. is supported by the Gertner Institute. H.S. acknowledges support by the Horizon 2020 European Research Council (ERC) Fund under the project MIRAGE 20-15 (Grant No. 639402). The authors acknowledge support from the Israel Science Foundation (ISF) Grant No. 1433/15 and the PAZY Young Investigator grant.

E.K. and H.G. contributed equally to this work.

APPENDIX: COMPOSITE PULSE FOR A ROBUST EQUAL SUPERPOSITION

An equal superposition between the two qubit states is realized when the rotation angle from Eq. (4) $\theta = \pi/2$. We focus on the shortest sequence with $N = 2$. Then, for the off-diagonal composite propagator element from Eq. (5) we have the condition

$$U_{12}^{(2)} = \frac{\frac{\Delta_1}{\Omega_1} - \frac{\Delta_2}{\Omega_2}}{\sqrt{\Delta_1^2 + \Omega_1^2}\sqrt{\Delta_2^2 + \Omega_2^2}} = -1/\sqrt{2}. \tag{A1}$$

We solve this equation for one of the independent parameters, $\frac{\Delta_1}{\Omega_1}$, and find that it is satisfied for $\frac{\Delta_1}{\Omega_1} = \frac{-1-\frac{\Delta_2}{\Omega_2}}{-1+\frac{\Delta_2}{\Omega_2}}$ and $\frac{\Delta_1}{\Omega_1} = \frac{-1+\frac{\Delta_2}{\Omega_2}}{1+\frac{\Delta_2}{\Omega_2}}$. We substitute this solution into the second derivative of $|U_{12}^{(2)}|^2$ with respect to A at $A = \pi$ and finds its roots. The exact expression is too cumbersome to be explicitly included here. Finally, we find the roots to be

$$\left(\frac{\Delta_1}{\Omega_1}, \frac{\Delta_2}{\Omega_2}\right) = \pm(-5.52, 0.69), \tag{A2}$$

which gives the interaction parameters of a two-pulse sequence that produces a robust equal superposition.

[1] M. Nielsen and I. Chuang, *Quantum Computation and Quantum Information* (Cambridge University Press, Cambridge, UK, 2000).
[2] E. L. Hahn, Phys. Rev. **80**, 580 (1950).
[3] H. Y. Carr and E. M. Purcell, Phys. Rev. **94**, 630 (1954).
[4] H. M. Cho, R. Tycko, A. Pines, and J. Guckenheimer, Phys. Rev. Lett. **56**, 1905 (1986).
[5] H. K. Cummins, G. Llewellyn, and J. A. Jones, Phys. Rev. A **67**, 042308 (2003).
[6] M. H. Levitt and R. Freeman, J. Magn. Reson. (1969) **33**, 473 (1979).
[7] R. Freeman, S. P. Kempsell, and M. H. Levitt, J. Magn. Reson. (1969) **38**, 453 (1980).
[8] M. H. Levitt, Prog. Nucl. Magn. Reson. Spectrosc. **18**, 61 (1986).
[9] R. Tycko, Phys. Rev. Lett. **51**, 775 (1983).
[10] B. T. Torosov and N. V. Vitanov, Phys. Rev. A **83**, 053420 (2011).
[11] B. T. Torosov, S. Guérin, and N. V. Vitanov, Phys. Rev. Lett. **106**, 233001 (2011).
[12] G. T. Genov, D. Schraft, T. Halfmann, and N. V. Vitanov, Phys. Rev. Lett. **113**, 043001 (2014).
[13] J. Keeler, *Understanding NMR Spectroscopy* (John Wiley and Sons, New York, 2005).
[14] A. A. Rangelov, N. V. Vitanov, and G. Montemezzani, Opt. Lett. **39**, 2959 (2014).
[15] A. A. Rangelov and E. Kyoseva, Opt. Commun. **338**, 574 (2015).
[16] E. Dimova, W. Huang, G. Popkirov, A. Rangelov, and E. Kyoseva, Opt. Commun. **366**, 382 (2016).
[17] I. Cohen, A. Rotem, and A. Retzker, Phys. Rev. A **93**, 032340 (2016).
[18] E. Kyoseva and N. V. Vitanov, Phys. Rev. A **88**, 063410 (2013).
[19] B. T. Torosov, E. S. Kyoseva, and N. V. Vitanov, Phys. Rev. A **92**, 033406 (2015).
[20] A. Politi, J. C. F. Matthews, and J. L. O'Brien, Science **325**, 1221 (2009).
[21] J. C. F. Matthews, A. Politi, A. Stefanov, and J. L. O'Brien, Nat. Photon. **3**, 346 (2009).
[22] R. J. Chapman, M. Santandrea, Z. Huang, G. Corrielli, A. Crespi, M.-H. Yung, R. Osellame, and A. Peruzzo, Nat. Commun. **7**, 11339 (2016).
[23] M. Frimmer and L. Novotny, Am. J. Phys. **82**, 947 (2014).
[24] G. Falci, A. D'Arrigo, A. Mastellone, and E. Paladino, Phys. Rev. Lett. **94**, 167002 (2005).
[25] E. Collin, G. Ithier, A. Aassime, P. Joyez, D. Vion, and D. Esteve, Phys. Rev. Lett. **93**, 157005 (2004).
[26] S. Takahashi, L. C. Brunel, D. T. Edwards, J. van Tol, G. Ramian, S. Han, and M. S. Sherwin, Nature (London) **489**, 409 (2012).
[27] T. Faust, J. Rieger, M. J. Seitner, J. P. Kotthaus, and E. M. Weig, Nat. Phys. **9**, 485 (2013).
[28] R. Hanson, O. Gywat, and D. D. Awschalom, Phys. Rev. B **74**, 161203(R) (2006).
[29] A. Yariv, IEEE, J. Quantum Electron. **9**, 9 (1973).